ACCOUNTS
of chemical research

Hyperthermal Oxidation of Graphite and Diamond

JEFFREY T. PACI,*,†,‡ TIMOTHY K. MINTON,§ AND GEORGE C. SCHATZ†

†Department of Chemistry, Northwestern University, 2145 Sheridan Road, Evanston, Illinois 60208-3113, United States, ‡Department of Chemistry, University of Victoria, P.O. Box 3065, Victoria, British Columbia V8W 3V6, Canada, and §Department of Chemistry and Biochemistry, Montana State University, Bozeman, Montana 59717, United States

RECEIVED ON DECEMBER 3, 2011

CONSPECTUS

Carbon materials have mechanical, electrical, optical, and tribological properties that make them attractive for use in a wide range of applications. Two properties that make them attractive, their hardness and inertness in many chemical environments, also make them difficult to process into useful forms. The use of atomic oxygen and other forms of oxidation has become a popular option for processing of these materials (etching, erosion, chemical functionalization, etc.). This Account provides an overview of the use of theory to describe the mechanisms of oxidation of diamond and graphite using hyperthermal (few electronvolts) oxygen atoms. The theoretical studies involve the use of Born–Oppenheimer molecular dynamics calculations in which on-the-fly electronic structure calculations have been performed using either density functional theory or density-functional-tight-binding semiempirical methods to simulate collisions of atomic oxygen with diamond or graphite. Comparisons with molecular-beam scattering on surfaces provide indirect verification of the results.

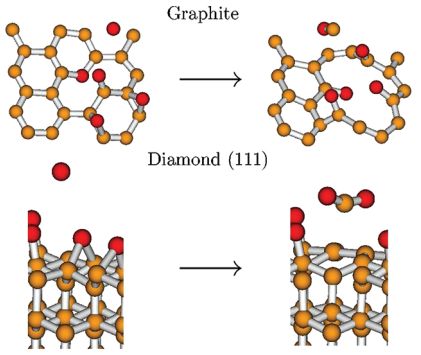

Adapted from Paci, J. T.; Upadhyaya, H.P.; Zhang, J.; Schatz, G. C.; Minton, T. K. *J. Phys. Chem. A* **2009**, *113*, 4677 and Shpilman, Z.; Gouzman, I.; Grossman, E.; Shen, L.; Minton, T. K.; Paci, J. T.; Schatz, G. C.; Akhvlediani, R.; Hoffman, A. *J. Phys. Chem. C* **2010**, *114*, 18996. Copyright 2009 and 2010 American Chemical Society.

Graphite surfaces become oxidized when exposed to hyperthermal atomic oxygen, and the calculations have revealed the mechanisms for formation of both CO and CO_2. These species arise when epoxide groups form and diffuse to holes on the surface where carbonyls are already present. CO and CO_2 form when these carbonyl groups dissociate from the surface, resulting in larger holes. We also discuss mechanisms for forming holes in graphite surfaces that were previously hole-free. For diamond, the (111) and (100) surfaces are oxidized by the oxygen atoms, forming mostly oxy radicals and ketones on the respective surfaces. The oxy-covered (111) surface can then react with hyperthermal oxygen to give gaseous CO_2, or it can become graphitized leading to carbon removal as with graphite. The (100) surface is largely unreactive to hyperthermal atomic oxygen, undergoing large amounts of inelastic scattering and supporting reactions that create O_2 or peroxy radicals. We did not observe a mechanism for the removal of carbon for this surface. These results are consistent with experimental studies that show formation of CO and CO_2 in graphite oxidation and preferential etching on (111) CVD diamond surfaces in comparison with (100) surfaces.

I. Introduction

Although there are exothermic reactions between O_2 and graphite that form CO and CO_2, graphite does not readily react in air at standard pressure and temperature. However, even for some high-quality graphites, temperatures as low as 600 °C can cause the onset of oxidation.[3] The processes involved during this oxidation have attracted significant research activity in recent years, because there has been renewed interest in the development of the next generation of nuclear fission power plants, with some of the new reactor technologies poised to benefit from the mechanical, thermal, and neutron-moderating properties of graphite.

Published on the Web 06/13/2012 www.pubs.acs.org/accounts
10.1021/ar200317y

Graphite is also an important lining material for industrial reactors operating at high temperature and pressure and is being studied as a surface material for rocket nozzles[4] and plasma diverters in nuclear fusion technologies.[5] Recently there has been significant interest in the oxidation of graphite into graphite oxide and in the development of graphene-based devices, where the ability to control oxidation is important.[6] Indeed, graphene can be oxidized directly and reversibly, using sources that contain atomic oxygen, the reversibility apparently allowing reduction without the creation of defects.[7] In addition, it is important to understand processes that result in the removal of carbon from graphitic materials because carbon removal is associated with the formation of defects, and the defects can have a significant impact on the properties of the remaining materials.

Kinoshita et al.[8] studied the chemical composition of a graphite surface after it was exposed, at room temperature, to hyperthermal atomic oxygen. X-ray photoelectron spectroscopy revealed the presence of C−O, C═O or O−C−O, and O−C═O. Many graphite oxidation reactions observed in the above-described systems are closely related to those that occur in combustion and gasification chemistry. Previous studies suggest that the rate-limiting step during the gasification of graphite is associated with a barrier height of ∼40 kcal/mol (1.7 eV)[9−11] and involves a reaction that at least initially produces CO (the CO may go on to form CO_2).[12,13] There is not yet a consensus on which reaction is associated with this barrier. However, there is strong evidence that it involves rearrangements in which epoxide groups move toward sheet edges or defects sites that are functionalized by carbonyls;[14,15] the carbonyls dissociate to produce a CO, and the epoxide groups move to form new C═O functional groups. There is also evidence that epoxide groups neighboring carbonyls weaken carbon−carbon bonds, facilitating the dissociation of the CO.[14,15] Graphitic dioxiranes are also of interest because their formation can provide a direct source of CO_2 (CO_2 produced without first producing CO).[9] It has been shown that the process is associated with a relatively low reaction barrier.[16]

Diamond is largely chemically inert, and it is the hardest known material. This makes the reliable removal of its surface layers a challenging problem. Nevertheless, it is important because the unique physical and electrical properties of diamond make it an attractive candidate for use in microelectronics. Polycrystalline chemically vapor-deposited diamond films often have rough surfaces and nonuniform thicknesses, which can adversely affect their suitability for use in applications.

Although quite erosion resistant, diamond thin films do erode when exposed to oxygen under certain sets of conditions. Reactive ion etching using oxygen-containing plasmas has been used to chemically etch polycrystalline diamond as a means of shaping and smoothing the material.[17−19] Similarly, oxygen plasmas have been used to etch single-crystal diamond,[20,21] with some of this work leading to a discussion of the need to find more anisotropic etching techniques.[22] Anisotropic etching in the context of this discussion refers to the preferential removal of atoms in a specific crystallographic direction. Its possibility has been demonstrated using a CO_2/H_2 plasma and in processes involving reactive-ion and microwave-plasma etching techniques.[23] Reference 24 indicates that a difference in (111) versus (100) diamond surface etch rates has been observed and is related to the effective stabilization of the (100) surface by oxygen functionalization. However, the authors provided limited details of the chemistry involved in the erosion of both of these surfaces.

Ion beam etching using beams that include oxygen or that collide with the sample in the presence of O_2 has also been used to etch diamond. Etch rates suggest that the presence of oxygen causes etching to occur chemically rather than by way of sputtering.[25,26] Other oxygen-containing gases have also been used.[27] Liquid oxidative etching using potassium nitrate has also been investigated.[24]

Static density functional theory (DFT) investigations of the types of structures that might result from the oxidation of the (100) and (111) surfaces have been performed. Details can be found in the Supporting Information.

High-quality diamond films are candidates for use in low-Earth orbit applications. This interest stems from their excellent mechanical and thermal properties, in particular, their resistance to oxidative erosion.[28,29] Such considerations are critical because $O(^3P)$ is the dominant driver of erosion in this region of Earth's atmosphere. In addition to its high concentration, this is also a result of its diradical character and the high energy (4.5 eV) at which collisions between the atoms and the leading edge of a spacecraft occur, due to their ∼7.4 km/s relative velocity. Other potentially useful carbon-based materials, such as graphite and diamond-like carbon, have significantly higher erosion rates when exposed to oxygen.[17] The difference between the diamond (111) and graphite erosion yields is about 2 orders of magnitude.[2] Oxidation is also important in the development of cutting tools and in preparing nanodiamonds for drug delivery applications.[30]

Recently a new direction of work on understanding the oxidation of carbon-containing materials has arisen through a combination of laboratory experiments,[31] which are capable of preparing beams of hyperthermal atomic oxygen, and theory,[32] which can directly simulate the dynamics of

these hyperthermal collisions using Born–Oppenheimer molecular dynamics methods. This Account provides an overview of the use of theory to describe diamond and graphite oxidation with an emphasis on the nature of the reaction mechanisms that occur, especially the mechanisms for forming gaseous species such as CO or CO_2 that remove carbon from the surfaces being exposed. Comparisons with experiments are included, which provide indirect evidence for the mechanisms observed, but the experiments have limited capabilities to sort out atomic level information, and ultimately it is the use of high-quality modeling that is crucial to generating meaningful insight and for extending this understanding to more conventional oxidation processes.

II. Methods and Models

Density functional theory has become a powerful tool for the computational scientist, providing a previously unavailable combination of accuracy and computational affordability. An introduction to the theory can be found in ref 33. Static simulations involving up to a few hundred atoms are now possible for DFT computer codes executed on modest modern serial computers. Dynamic simulations, with forces and energies calculated using DFT single-point calculations, for simulations lasting up to picoseconds are also possible. Density functional-based tight-binding (DFTB) is a semiempirical method, parametrized using DFT simulations. When implemented in its self-consistent charge (SCC) form, it maintains much of the accuracy of full-blown DFT at a fraction of the computational cost. The method has been recently reviewed in ref 34.

To investigate the oxidation of graphite surfaces, direct dynamics calculations were performed based on DFT. The Perdew–Burke–Ernzerhof (PBE)[35] functional with a double-ζ plus polarization (DZP) basis set was used.[33] Models were based on a 24-atom graphene sheet.

Larger numbers of atoms were necessary to accurately model diamond surfaces. Models consisting of 72 carbon atoms were used to investigate the oxidation of (100) and (111) surfaces, forming slabs with six atomic layers. The numbers of atoms meant that only a small number of PBE/DZP trajectories were computationally affordable. The use of this method was the limiting factor in the model sizes that could be considered. Larger numbers of trajectories were run based on SCC-DFTB. Periodic boundary conditions (PBC) were used in all of the simulations.

A pristine graphene sheet and sheets containing a single-atom vacancy defect were studied. A pristine sheet functionalized with eight oxygen atoms was created to explore the behavior of sheets without preexisting holes. We also chose

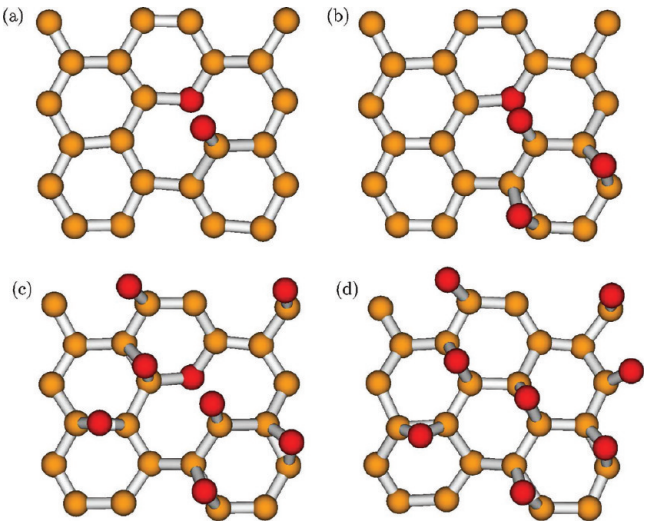

FIGURE 1. The precollision graphene structures: A sheet containing a single-atom vacancy defect and (a) two oxygen atoms (model A), (b) four oxygen atoms (model B), or (c) eight oxygen atoms (model C). Panel d shows a pristine sheet functionalized with eight oxygen atoms (model D). Carbon atoms are light yellow and oxygen atoms are dark red. Reproduced with permission from ref 1. Copyright 2009 American Chemical Society.

to examine a single-atom vacancy, because it is one of the next-simplest structures that could be considered. Because dangling bonds are not likely to exist for extended periods of time in an oxygen-rich environment, we capped their valencies with oxygen atoms.

The structure shown in Figure 1a illustrates how the valencies at the single-atom vacancy were satisfied. This structure, which contains two oxygen atoms, is based on a frequently found structure in our recent Monte Carlo and molecular dynamics (MD) simulations of graphite oxide.[36] It contains a carbonyl group, which is known from combustion chemistry to be important at holes in and at the edges of graphene sheets.[14,15] The structure will be referred to as model A. Motivated by the work in refs 14 and 15, we also investigated the structure shown in Figure 1b (model B).

Additional oxygen atoms were added to the sheet to create the models shown in Figure 1c,d (models C and D). Their positions were selected at random from all of the remaining physically realistic sites for oxygen atoms sitting atop carbon atoms and oxygen atoms in epoxide positions on the surface side of the sheet. Note that because of the PBC, the oxygen atoms in models C and D at the edges of the sheets, which appear to be attached to the sheets by only one bond, are in fact attached by two bonds. There are no atop oxygen atoms in models C or D. Although they were present in the structures before geometry optimization, in all cases they relaxed to form epoxide groups.

Preoxidation was also performed on some of the diamond surfaces. A fluence of 6×10^{19} O atoms per square centimeter (accumulated in ~3.5 h) is typical of those used in the diamond experiments such as those described in ref 2. This corresponds to a fluence of 6×10^{3} O atoms per square angstrom and can be compared with the fluence in a trajectory that is 1.3×10^{-2} O atoms Å^{-2}. To rectify the disparity between experimental and calculated fluences, we consider surfaces that are preoxidized to various levels, including surfaces that are close to steady state in oxygen coverage. A large number of trajectories were propagated, with different surface functionalizations, as described in section IV.

Intramolecular trajectories were run for each model, before exposing them to a colliding oxygen atom. The trajectories were randomly sampled, in order to provide a set of initial atomic positions and velocities for the direct dynamics trajectories.

Sheets and slabs were exposed to O(^{3}P) atoms traveling with 5 eV of kinetic energy, approximately matching the collision energies used in a number of experiments.[1,2,37−39] It is unlikely that an oxygen atom with a collision energy of 5 eV would result in the removal of one or more carbon atoms from an unfunctionalized hole-free graphene sheet, so we studied the functionalized structures shown in Figure 1. Normal incidence with the model surfaces was considered, with impact locations chosen at random. Each graphene-based direct dynamics calculation was performed twice, with each set of initial conditions run once in the lowest-energy singlet and once in lowest-energy triplet electronic state. One hundred singlet and one hundred triplet trajectories were run, for each of the four models.

For the diamond trajectories, electron spin was free to become polarized, but the total spin of the slab (oxidized or otherwise) plus the incoming O atom was fixed at two spin-up electrons, that is, the system evolved in the lowest-energy triplet electronic state. Spin−orbit interactions were not included, but in our past studies, we have not found this to play an important role for high-energy collisions.[1] In an extended system, it is still possible for spin flips to occur.

Additional simulation method details can be found in the Supporting Information.

III. Graphite

A variety of reactions were observed in O + graphite trajectories for each of the models shown in Figure 1. Some of the more interesting reactions are summarized in Table 1. Aside from the observation of slightly different numbers of singlet versus triplet reactive events, the type of reactivity observed in both trajectory types was the same, so the results have been combined in the table.

TABLE 1. Some of the Reactions Observed during Trajectories That Were Run on the Lowest-Energy Singlet and Lowest-Energy Triplet Potential-Energy Surfaces[a]

reaction	model A	model B	model C	model D
ring opening	68	26	25	0
epoxide formation	151	147	62	24
epoxide migration	58	80	33	38
tethered carbonyl	5	1	0	0
O_2 formation	1	34	108	155
CO_2 formation	0	4	3	0
CO formation	0	1	6	0
dioxirane formation	0	2	2	0
inelastic O	0	7	14	4
sheet damage	0	0	0	5

[a]One hundred trajectories were propagated for each model on each surface. Results for the four models described in Figure 1 are shown, and the results for both surfaces have been combined in the table. The numbers of trajectories in which each reaction was observed are shown. The totals for each column sum to more than two hundred because multiple reactions occurred during some of the trajectories. See the text for details beyond the abbreviated descriptions of the reactions provided in the first column.

Epoxide formation is a highly probable event, particularly at low oxygen surface concentrations. As the surface becomes increasingly covered by these groups, the probability of O_2 formation increases. The fact that epoxide formation occurs more than half of the time for the coverage shown in model B and less than half of the time for model C, combined with the fact that O_2 formation occurs in less than half of the model B trajectories and more than half of the model C trajectories suggests that the equilibrium concentration of surface oxygen is probably between those shown in models B and C. Nearly all of the reactions producing O_2 did so by way of an Eley−Rideal (direct) mechanism, a finding that is consistent with experimental observations.[1]

Among the other reactions in Table 1 are the following: (1) ring opening, the breaking of a C−O bond in the oxygen-containing six-membered ring; (2) epoxide migration, the movement of an oxygen atom from one epoxide location to another; the oxygen atom moves atop a carbon atom in the process, sometimes lingering there for tens of femtoseconds; (3) tethered carbonyl, a CO group attached to the sheet by one bond to its carbon atom; (4) inelastic O, the incoming oxygen atom undergoes an inelastic collision with the surface and then scatters away; (5) sheet damage, the breaking of a C−C bond in the hole-free sheet. Undefected graphite, regardless of its level of oxidation, is resistant to damage by thermal O or O_2, but the sheet damage mechanism suggests that this is not true for hyperthermal O. Note that model D, which shows sheet damage, has higher than what we estimate is the steady-state oxygen

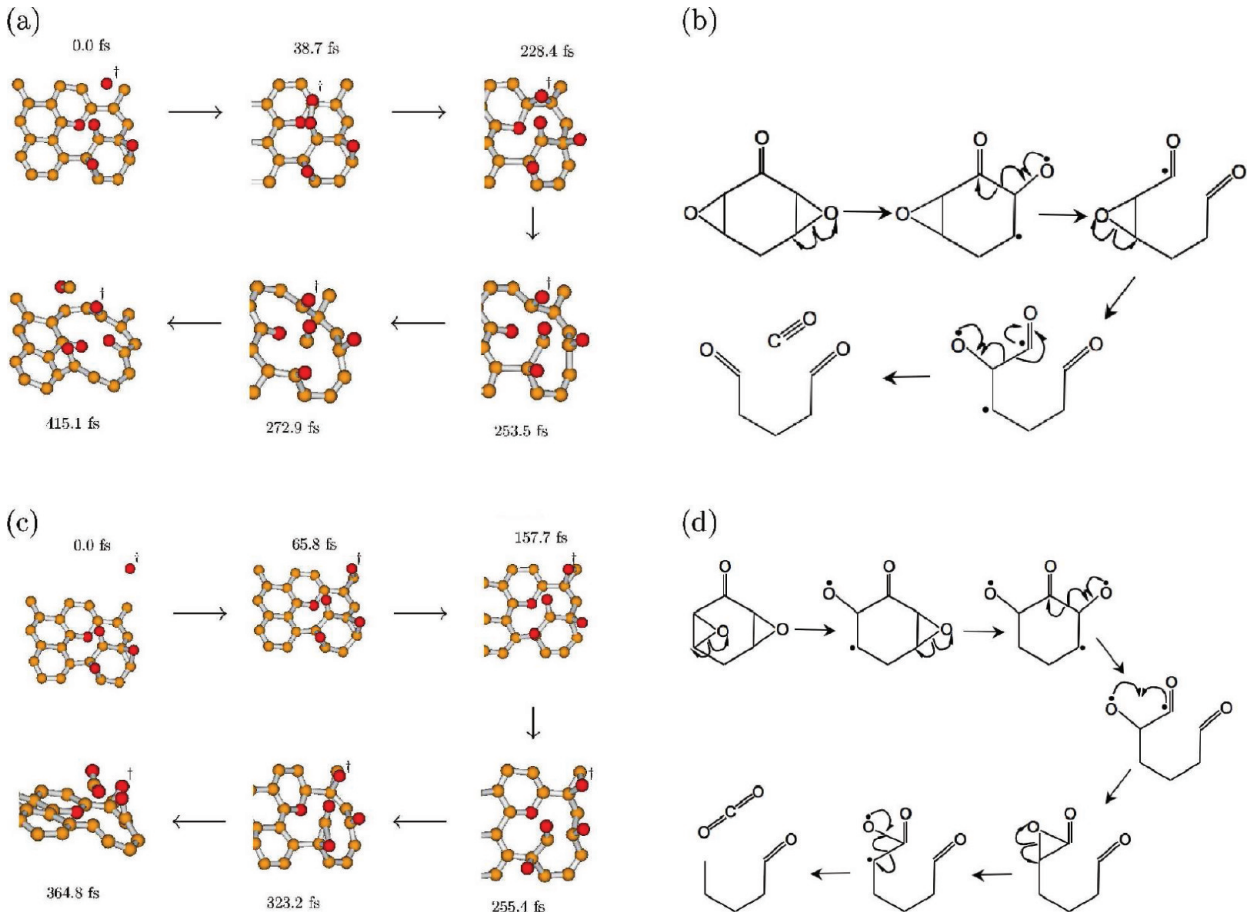

FIGURE 2. Reactions producing CO, panel a, and CO_2, panel c, from graphitic surfaces. To help guide the eye, the incoming oxygen atom is labeled with a "†". See the text for descriptions of the details of the trajectories. Note that in some panels, only part of the graphene sheet is shown. Also in many cases, it was rotated. Both were done in order to provide a better view of the areas involved in and adjacent to the reaction of interest. Electron pushing diagrams associated with the two trajectories are also shown panels b and d. Panels a and c were reproduced with permission from ref 1. Copyright 2009 American Chemical Society.

atom coverage, so this likely overestimates the hole formation probability.[1]

Two additional carbonyl groups, each attached to sheets by two bonds to their respective carbon atoms, were formed in 76.5% of the model B and C trajectories (those with coverages close to what one expects experimentally), in which oxygen-containing ring opening was observed. The incidence with which these carbonyl pairs were formed is not summarized in the table. These reactions are important because it is a carbonyl that is almost always involved in the formation of CO/CO_2. Details of the mechanisms involved in producing CO/CO_2 will be discussed below. Also, when holes were created in the model D sheets, they were accompanied by the formation of a pair of carbonyl groups at the hole edges. This process suggests that not only can holes be created in previously hole-free graphite by hyperthermal O atoms but also the process results in the formation of functional groups that tend to facilitate the removal of carbon from the surface upon subsequent O-atom collision. The migration of epoxide groups is a probable event as the table shows, and it has been observed to bring epoxides into positions adjacent to carbonyl groups.[1,36] As discussed in section I, epoxides neighboring carbonyl groups are thought to lower the barrier to dissociation of carbonyl groups.[14,15]

The other reactions observed during the trajectories are discussed in ref 1 and its associated Supporting Information.

The trajectories suggest mechanisms by which carbon can be removed from the surface of graphite. As indicated in the table, both CO and CO_2 were observed. Figure 2, panels a and b, shows a reaction that resulted in the creation of CO from the surface side of the graphene sheet. As illustrated in Figure 2a, the incoming oxygen atom struck the oxygen atom in the carbonyl group (38.7 fs), vibrationally exciting the sheet and forming an epoxide group. Two epoxide groups neighboring the carbonyl then moved atop carbon atoms neighboring the carbonyl (228.4 fs). The sequential

breaking of two carbon−carbon bonds released the CO and produced two new carbonyl groups (253.5−415.1 fs). As mentioned previously, this type of reaction is also thought to play an important role in combustion chemistry,[14,15] so this reaction was not unexpected.

An electron pushing diagram illustrating a plausible reaction mechanism is shown in Figure 2b. The repeated formation of oxy radicals and C=O bonds results in the release of CO in a process that is analogous to β-scission.[40] Note that two unpaired electrons were added to the sheet during the bonding of the incoming O(^{3}P) atom and that graphene is a semimetal, so unpaired electrons do not need to stay localized at the positions on the sheets where they are initially located. For example, two unpaired electrons move into the sheet during the processes shown in Figure 2b.

We also identified a reaction that resulted in the creation of CO_2 from the graphene sheet. The early stages of the mechanism (see Figure 2, panels c and d) are similar to those described in relation to the mechanism for the release of CO shown in Figure 2, panels a and b. In the CO_2 case, the impact of the incoming oxygen atom occurred close to the pair of epoxides neighboring the carbonyl. Note that because of the PBC, a collision near the top right of the sheet is "close to" the atoms at the bottom right of the sheet. The epoxide oxygen atoms flipped atop respective carbon atoms (157.7 fs) that neighbor the carbonyl group. One carbon−carbon bond to the carbonyl broke (255.4 fs), and instead of leaving the sheet alone, the nascent CO molecule became bonded to a neighboring atop oxygen atom (323.2 fs). It then departed the sheet as a CO_2 molecule (364.8 fs).

An electron pushing diagram illustrating a plausible reaction mechanism is shown in Figure 2d. As in the CO case, the repeated formation of oxy radicals and C=O bonds results in the release of a carbon atom, in a process that is analogous to β-scission.

Two other mechanisms resulting in the release of a CO_2 molecule from the sheet were also characterized. One involved the formation of a ring that changed the hybridization of the carbonyl carbon atom from sp^2 to sp^3. The process leaves what was originally the carbonyl oxygen atom as a radical, making it susceptible to attack by the CO molecule that removed it as the CO departed. In the other, the incoming oxygen atom collided with the carbonyl group forming a dioxirane. The species led to the breaking of the two carbon−carbon bonds tethering it to the sheet, and went on to form CO_2. Additional details of these mechanisms can be found in ref 1.

The experimental studies of hyperthermal oxygen atom collisions with graphite[1,37] provide only limited information to confirm the results that we have described. In these studies, it was found that both CO and CO_2 molecules are produced.[1] The incident O-atom angle used in the experiments was 45°, yet most of the molecules scatter approximately normal to the surface. This is consistent with the complex reaction mechanisms described above, which are expected to result in CO/CO_2 receding from the surface in the direction of the surface normal on average, regardless of the incident angle. In experiments at 493 K, about 10% of the incident oxygen atoms are converted into these species.[39] Also, we observed five hole formation events in sheets previously without holes at a flux of 1.5×10^{16} O atoms cm^{-2}. This flux is small compared with those sometimes used experimentally, which can be on the order of 10^{20} O atoms cm^{-2}. Under experimental conditions similar to those used in our trajectory studies, O-atom exposure converts the smooth surface of graphite into a tower- and hillock-covered structure.[37] This is consistent with a high rate of new hole formation.

Reactive force fields have also been used to theoretically examine the graphene sheets shown in Figure 1.[41] The results, in terms of the number of occurrences of various reactive events, compare reasonably well with those reported above. Sheet damage, resulting in the formation of carbonyl groups, and CO_2 formation were significantly more probable when the force field was used. CO formation was less probable. The computational affordability of force field methods made it possible to also explore larger graphitic sheets.[41] Twenty-five times expanded sheets initially without holes were examined. The steady state oxygen atom coverage was found to be more than one oxygen atom per three carbon atoms, somewhat higher than the DFT-based estimate. More inelastic scattering and epoxide formation, and less epoxide migration, O_2 and CO_2 formation, and sheet damage were observed for the larger compared with the smaller model when the force field was used. The types of reactivity predicted using the two methods and model sizes were the same. Kinks in the larger sheets were also observed, a result that may have been influenced by the single-layer nature of the simulations. Sheet break-up upon exposure to multiple oxygen atom collisions with bilayer graphene was reported, although the role played by the associated dramatic increase in temperature warrants additional study.

IV. Diamond

There is now atomic force microscope-based evidence for the selective etching of diamond facets by hyperthermal

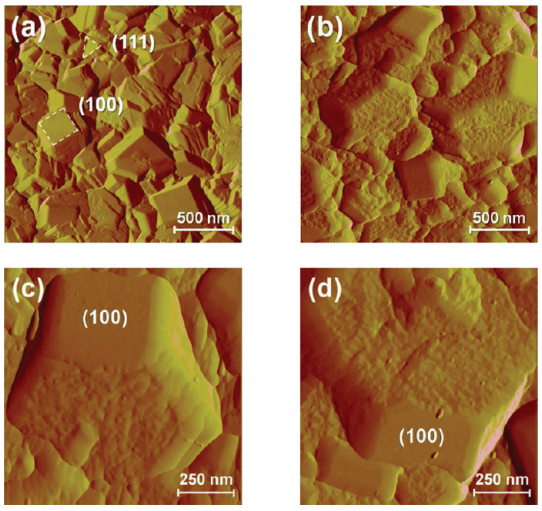

FIGURE 3. AFM images of polycrystalline diamond film before (a) and after (b–d) exposure to a fluence of 6×10^{19} O atoms cm^{-2} of 5 eV atomic oxygen. The (100) and (111) facets are delineated in panel a. Reproduced with permission from ref 2. Copyright 2010 American Chemical Society.

oxygen, images of which are shown in Figure 3.[2] The images show the surface of a diamond thin film grown by chemical vapor deposition. The films are polycrystalline, and their surfaces are composed of a variety of exposed facets. The (100) and (111) facets tend to be square and triangular, respectively (see Figure 3a).[42] Exposure to 5 eV oxygen atoms results in the erosion of all but the (100) facets (see Figure 3b–d). We used trajectory studies to investigate the reactivity of (100) and (111) surface facets, to explore the experimentally observed differences in etch rates.[2,43]

The simulations indicate that the hydrogen atoms that are expected to terminate the diamond (111) and (2×1)-reconstructed (100) surfaces and are expected to exist at the end of the growth process are readily removed by the oxygen atoms. As the hydrogen is removed, additional oxygen atoms tend to form ketones on the (100) surfaces and oxy radicals on (111). The steady-state oxygen atom coverages were estimated as the concentrations at which the probability of an incoming oxygen atom removing an oxygen atom already on the surface is equal to the probability of an incoming atom being adsorbed. For the (111) surface, this corresponded to ~0.67 O atoms per surface carbon atom. For the (100) surface, which loses its (2×1) reconstruction, the steady-state coverage corresponded to nearly complete coverage with ketones.

At its steady state coverage, the (111) surface is prone to partial graphitization. Such a process took place in ~5% of the trajectories and was characterized by the breaking of a carbon–carbon bond between the second and third carbon

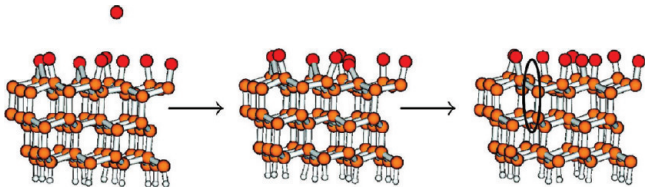

FIGURE 4. Hyperthermal oxygen atom collisions can cause a partial graphitization of the diamond (111) surface. The incoming oxygen atom (left panel) becomes bound to the surface as an oxy radical (center panel) and causes the collision-induced dissociation of a neighboring carbon–carbon bond. The location of the broken bond is indicated by the ellipse. Reproduced with permission from ref 2. Copyright 2010 American Chemical Society.

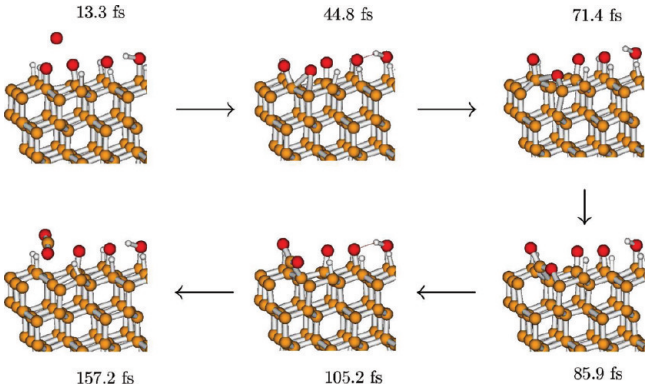

FIGURE 5. Reaction producing CO_2 from an O-atom collision with an oxidized (111) diamond surface, as illustrated using snapshots from a PBE/DZP-based trajectory. Following arrows clockwise: The incoming O atom (13.3 fs) collided with an atop O atom, pushing it aside (44.8 fs). The force of the collision broke a C–C bond, with the incoming O atom adding itself to the surface, forming an ether (71.4 fs). Another C–C bond broke (85.9 fs), followed by an O–C ether bond (105.2 fs). Finally, a C–C bond broke, releasing a CO_2 molecule (157.2 fs). Reproduced with permission from ref 43. Copyright 2011 American Chemical Society.

layers, bringing the carbon atom from the second layer into the plane of the first. Snapshots from an example of such a trajectory are shown in Figure 4. The change seems to be such that the reverse process would require the surmounting of a significant energy barrier. In a previous study,[1] it has been shown that graphite is quickly eroded by a 5 eV oxygen-atom beam, as the discussion in the previous section suggests, so this graphitization process is expected to leave the surface susceptible to erosion during subsequent O-atom collisions. Note that it is possible that the propensity for graphitization is related to the thickness of the slab.[2]

Even without graphitization, the (111) surface is prone to the direct removal of carbon as CO_2 molecules. Figure 5 shows snapshots from a trajectory that illustrate one such mechanism. The surface coverage in this case contains some hydrogen and was designed to simulate the surface chemistry shortly after diamond is first exposed to

5 eV O(^{3}P). As is indicated in the figure, a CO_2 molecule was released from the surface within ~120 fs of the oxygen atom colliding with the surface. A similar reaction was also observed in a trajectory propagated with slightly less than the steady-state coverage (six instead of eight precollision surface oxygen atoms per 12 first-layer carbon atoms). Finally, the production of a tethered CO_2 molecule was observed in a trajectory like the one shown in the 85.9 fs panel of Figure 5. Present at the end of this particular trajectory, the fact that such a structure went on to produce CO_2 in the trajectory shown in Figure 5 suggests that the barrier to dissociation of a CO_2 molecule from such a structure is not large. Thus, this surface damage also suggests a mechanism for the removal of carbon from the (111) surface. All three of these mechanisms were driven by β-scission-like processes.[43]

In contrast to the (111) surface, no mechanism for the removal of carbon from the (100) surface was observed at its steady-state coverage. In the SCC-DFTB-based simulations, inelastic scattering from the ketone-covered surface was the most probable collision event (see Figure 10 of ref 2). A dioxirane was formed, but unlike its graphitic analogue, it is not expected to be associated with a particularly low barrier to CO_2 release. A partially detached carbonyl group was formed in one of the trajectories. However, given sufficient time, the group will reform a ketone. The ketone reformation would remove four dangling bonds, so it would almost certainly be barrierless. This damage suggests that the layer-by-layer erosion of the (100) surface may be possible. However, the lack of a mechanism for carbon removal suggests that the (100) surface is more erosion resistant than the (111) surface. The PBE/DZP-based trajectories showed slightly different behavior. In this case, collisions with the ketone-covered (100) surface most often resulted in the formation of O_2 or peroxy radicals. Ketones were sometimes converted to ether groups as a result of the collisions. Nevertheless, no mechanism for the removal of carbon from the (100) surface was observed. Differences in the approximations that enter the Hamiltonians associated with the PBE/DZP versus SCC-DFTB methods are the reason for these differences in behavior.

A summary of the reactions observed during the trajectories and a discussion of Pandey reconstruction can be found in the Supporting Information.

V. Conclusion

Carbon materials have attracted a seemingly ever-increasing amount of research interest over the last 2 decades. Diamond thin films and materials composed of and closely related to graphite are routinely considered for a broad range of applications because of their numerous exceptional properties. For most applications, it is necessary to further process these materials after their initial manufacture. In this Account, we described the results of the use of quantum-mechanical-based direct dynamics to explore the use of hyperthermal atomic oxygen atoms for the oxidation of graphite and diamond. The technique suggested several mechanisms by which carbon can be removed from graphite, forming CO and CO_2 when it is exposed to such atoms. Carbonyl groups at holes and epoxide migration play important roles. Also, hyperthermal oxygen atoms can cause new holes to form, which become functionalized by carbonyl groups and thus can become sources of additional CO/CO_2 upon subsequent O-atom collisions. The diamond (111) surface is also eroded by hyperthermal oxygen atoms. It becomes functionalized by oxy radicals and is susceptible to graphitization, which can lead to the removal of carbon. Mechanisms for the direct removal of carbon as part of CO_2 from the (111) surface were also characterized. The (100) surface, nearly fully covered by ketones and ethers at its steady-state coverage, seems to be able to resist erosion when exposed to hyperthermal oxygen atoms. The simulations showed no mechanism for the removal of carbon from this surface.

This work was supported by grants from the National Science Foundation (Nos. CHE-0943639 and CMMI-0856492), ARO MURI grant No. W911NF-09-1-0541, and AFOSR (Nos. FA9550-10-1-0205 and FA9550-10-1-0563). We thank Jeremy E. Wulff for valuable discussions.

Supporting Information. Static density functional theory simulations, additional simulation method details, and summary of diamond-surface reactions and Pandey reconstruction. This material is available free of charge via the Internet at http://pubs.acs.org.

BIOGRAPHICAL INFORMATION

Jeffrey T. Paci received a B.Sc. in Chemical Physics from the University of Toronto in 1992 and a Ph.D. in Chemistry from Queen's University in 2002. He is currently a Postdoctoral Fellow with Prof. George C. Schatz at Northwestern University and a Visiting Scientist at the University of Victoria.

Timothy K. Minton is a Professor of Chemistry & Biochemistry at Montana State University. He received his B.S. in Chemistry from the University of Illinois at Urbana–Champaign in 1980 and his Ph.D. in Chemistry in 1986 from the University of California at Berkeley.

George C. Schatz is a Professor of Chemistry at Northwestern University. He received his B.S. in Chemistry from Clarkson University in 1971 and his Ph.D. in Chemistry in 1976 from Caltech.

FOOTNOTES

The authors declare no competing financial interest.

REFERENCES

1 Paci, J. T.; Upadhyaya, H. P.; Zhang, J.; Schatz, G. C.; Minton, T. K. Theoretical and Experimental Studies of the Reactions Between Hyperthermal O(^{3}P) and Graphite: Graphene-Based Direct Dynamics and Beam-Surface Scattering Approaches. *J. Phys. Chem. A* **2009**, *113*, 4677–4685.

2 Shpilman, Z.; Gouzman, I.; Grossman, E.; Shen, L.; Minton, T. K.; Paci, J. T.; Schatz, G. C.; Akhvlediani, R.; Hoffman, A. Oxidation and Etching of CVD Diamond by Thermal and Hyperthermal Atomic Oxygen. *J. Phys. Chem. C* **2010**, *114*, 18996–19003.

3 Blyholder, G.; Eyring, H. Kinetics of Graphite Oxidation. *J. Phys. Chem.* **1957**, *61*, 682–688.

4 Keswani, S. T.; Andiroglu, E.; Campbell, J. D.; Kuo, K. K. Recession Behavior of Graphitic Nozzles in Simulated Rocket Motors. *J. Spacecr. Rockets* **1985**, *22*, 396–397.

5 Federici, G.; Skinner, C. H.; Brooks, J. N.; Coad, J. P.; Grisolia, C.; Haasz, A. A.; Hassanein, A.; Philipps, V.; Pitcher, C. S.; Roth, J.; Wampler, W. R.; Whyte, D. G. Plasma-Material Interactions in Current Tokamaks and Their Implications for Next Step Fusion Reactors. *Nucl. Fusion* **2001**, *41*, 1967–2137.

6 Zhu, Y. W.; Murali, S.; Cai, W. W.; Li, X. S.; Suk, J. W.; Potts, J. R.; Ruoff, R. S. Graphene and Graphene Oxide: Synthesis, Properties, and Applications. *Adv. Mater.* **2010**, *22*, 3906–3924.

7 Hossain, M. Z.; Johns, J. E.; Bevan, K. H.; Karmel, H. J.; Liang, Y. T.; Yoshimoto, S.; Mukai, K.; Koitaya, T.; Yoshinobu, J.; Kawai, M.; Lear, A. M.; Kesmodel, L. L.; Tait, S. L.; Hersam, M. C. Chemically Homogeneous and Thermally Reversible Oxidation of Epitaxial Graphene. *Nat. Chem.* **2012**, *4*, 305–309.

8 Kinoshita, H.; Umeno, M.; Tagawa, M.; Ohmae, N. Hyperthermal Atomic Oxygen Beam-Induced Etching of HOPG (0001) Studied by X-Ray Photoelectron Spectroscopy and Scanning Tunneling Microscopy. *Surf. Sci.* **1999**, *440*, 49–59.

9 Stevens, F.; Kolodny, L. A.; Beebe, T. P., Jr. Kinetics of Graphite Oxidation: Monolayer and Multilayer Etch Pits in HOPG Studied by STM. *J. Phys. Chem. B* **1998**, *102*, 10799–10804.

10 Backreedy, R.; Jones, J. M.; Pourkashanian, M.; Williams, A. A Study of the Reaction of Oxygen with Graphite: Model Chemistry. *Faraday Discuss.* **2001**, *119*, 385–394.

11 Hahn, J. R. Kinetic Study of Graphite Oxidation Along Two Lattice Directions. *Carbon* **2005**, *43*, 1506–1511.

12 Hall, P. J.; Calo, J. M. Secondary Interactions Upon Thermal-Desorption of Surface Oxides from Coal Chars. *Energy Fuels* **1989**, *3*, 370–376.

13 Incze, A.; Pasturel, A.; Chatillon, C. Oxidation of Graphite by Atomic Oxygen: A First-Principles Approach. *Surf. Sci.* **2003**, *537*, 55–63.

14 Chen, N.; Yang, R. T. Ab Initio Molecular Orbital Study of the Unified Mechanism and Pathways for Gas-Carbon Reactions. *J. Phys. Chem. A* **1998**, *102*, 6348–6356.

15 Montoya, A.; Mondragón, F.; Truong, T. N. Formation of CO Precursors During Char Gasification with O_2, CO_2 and H_2O. *Fuel Process. Technol.* **2002**, *77*, 125–130.

16 Sánchez, A.; Mondragón, F. Role of the Epoxy Group in the Heterogeneous CO_2 Evolution in Carbon Oxidation Reactions. *J. Phys. Chem. C* **2007**, *111*, 612–617.

17 Joshi, A.; Nimmagadda, R. Erosion of Diamond Films and Graphite in Oxygen Plasma. *J. Mater. Res.* **1991**, *6*, 1484–1490.

18 Roppel, T.; Ramesham, R.; Ellis, C.; Lee, S. Y. Thin-Film Diamond Microstructures. *Thin Solid Films* **1992**, *212*, 56–62.

19 Sirineni, G. M. R.; Naseem, H. A.; Malshe, A. P.; Brown, W. D. Reactive Ion Etching of Diamond as a Means of Enhancing Chemically-Assisted Mechanical Polishing Efficiency. *Diamond Relat. Mater.* **1997**, *6*, 952–958.

20 Sandhu, G. S.; Chu, W. K. Reactive Ion Etching of Diamond. *Appl. Phys. Lett.* **1989**, *55*, 437–438.

21 Ando, Y.; Nishibayashi, Y.; Sawabe, A. `Nano-Rods' of Single Crystalline Diamond. *Diamond Relat. Mater.* **2004**, *13*, 633–637.

22 Koslowski, B.; Strobel, S.; Herzog, T.; Heinz, B.; Boyen, H. G.; Notz, R.; Ziemann, P. Fabrication of Regularly Arranged Nanocolumns on Diamond (100) Using Micellar Masks. *J. Appl. Phys.* **2000**, *87*, 7533–7538.

23 Nishibayashi, Y.; Ando, Y.; Saito, H.; Imai, T.; Hirao, T.; Oura, K. Anisotropic Etching of a Fine Column on a Single Crystal Diamond. *Diamond Relat. Mater.* **2001**, *10*, 1732–1735.

24 de Theije, F. K.; van Veenendaal, E.; van Enckevort, W. J. P.; Vlieg, E. Oxidative Etching of Cleaved Synthetic Diamond {111} Surfaces. *Surf. Sci.* **2001**, *492*, 91–105.

25 Whetten, T. J.; Armstead, A. A.; Grzybowski, T. A.; Ruoff, A. L. Etching of Diamond with Argon and Oxygen Ion-Beams. *J. Vac. Sci. Technol. A* **1984**, *2*, 477–480.

26 Leech, P. W.; Reeves, G. K.; Holland, A.; Shanks, F. Ion Beam Etching of CVD Diamond Film in Ar, Ar/O_2 and Ar/CF_4 Gas Mixtures. *Diamond Relat. Mater.* **2002**, *11*, 833–836.

27 Efremow, N. N.; Geis, M. W.; Flanders, D. C.; Lincoln, G. A.; Economou, N. P. Ion-Beam-Assisted Etching of Diamond. *J. Vac. Sci. Technol. B* **1985**, *3*, 416–418.

28 Gregory, J. C.; Peters, P. N.; Swann, J. T. Effects on Optical Systems from Interactions with Oxygen Atoms in Low Earth Orbit. *NASA TM 100459* **1988**, *2*, 2-1–2-12.

29 Gregory, J. C.; Peters, P. N. The Reaction of 5 eV Oxygen Atoms with Polymeric and Carbon Surfaces in Earth Orbit. *NASA TM 100459* **1988**, *2*, 4-1–4-5.

30 Adnan, A.; Chen, H.; Lee, J.; Schaffer, D. J.; Barnard, A. S.; Schatz, G. C.; Ho, D.; Liu, W. -K. Atomistic Simulation and Measurement of pH Dependent Cancer Therapeutic Interactions with Nanodiamond Carrier. *Mol. Pharmaceutics* **2011**, *8*, 368–374.

31 Minton, T. K.; Garton, D. J. Dynamics of Atomic-Oxygen-Induced Polymer Degradation in Low-Earth Orbit. In *Chemical Dynamics in Extreme Environments*; Dressler, R. A., Ed.; Advanced Series in Physical Chemistry 11; World Scientific: Singapore, 2001; pp 420−489.

32 Troya, D; Schatz, G. C. Hyperthermal Chemistry in the Gas Phase and on Surfaces: Theoretical Studies. *Int. Rev. Phys. Chem.* **2004**, *23*, 341–373.

33 Jensen, F. *Introduction to Computational Chemistry*, 2nd ed.; John Wiley & Sons Ltd.: Chichester, West Sussex, 2007.

34 Frauenheim, T.; Seifert, G.; Elstner, G. S. M.; Niehaus, T.; Köhler, C.; Amkreutz, M.; Sternberg, M.; Hajnal, Z.; Carlo, A. D.; Suhai, S. Atomistic Simulations of Complex Materials: Ground-State and Excited-State Properties. *J. Phys.: Condens. Matter* **2002**, *14*, 3015–3047.

35 Perdew, J. P.; Burke, K.; Ernzerhof, M. Generalized Gradient Approximation Made Simple. *Phys. Rev. Lett.* **1996**, *77*, 3865–3868.

36 Paci, J. T.; Belytschko, T.; Schatz, G. C. Computational Studies of the Structure, Behavior Upon Heating, and Mechanical Properties of Graphite Oxide. *J. Phys. Chem. C* **2007**, *111*, 18099–18111.

37 Nicholson, K. T.; Minton, T. K.; Sibener, S. J. Temperature-Dependent Morphological Evolution of HOPG Graphite Upon Exposure to Hyperthermal O(^{3}P) Atoms. *Prog. Org. Coat.* **2003**, *47*, 443–447.

38 Nicholson, K. T.; Sibener, S. J.; Minton, T. K. Nucleation and Growth of Nanoscale to Microscale Cylindrical Pits in Highly-Ordered Pyrolytic Graphite Upon Hyperthermal Atomic Oxygen Exposure. *High Perform. Polym.* **2004**, *16*, 197–206.

39 Nicholson, K. T.; Minton, T. K.; Sibener, S. J. Spatially Anisotropic Etching of Graphite by Hyperthermal Atomic Oxygen. *J. Phys. Chem. B* **2005**, *109*, 8476–8480.

40 March, J. *Advanced Organic Chemistry: Reactions, Mechanisms and Structure*, 3rd ed.; John Wiley & Sons: Hoboken, NJ, 1985.

41 Srinivasan, S. G.; van Duin, A. C. T. Molecular-Dynamics-Based Study of the Collisions of Hyperthermal Atomic Oxygen with Graphene Using the ReaxFF Reactive Force Field. *J. Phys. Chem. C* **2011**, *115*, 13269–13280.

42 Silva, F.; Bonnin, X.; Achard, J.; Brinza, O.; Michau, A.; Gicquel, A. Geometric Modeling of Homoepitaxial CVD Diamond Growth: I. The {100}{111}{110}{113} System. *J. Cryst. Growth* **2008**, *310*, 187–203.

43 Paci, J. T.; Schatz, G. C.; Minton, T. K. Theoretical Studies of the Erosion of (100) and (111) Diamond Surfaces by Hyperthermal O(^{3}P). *J. Phys. Chem. C* **2011**, *115*, 14770–14777.